

AD-R163 171

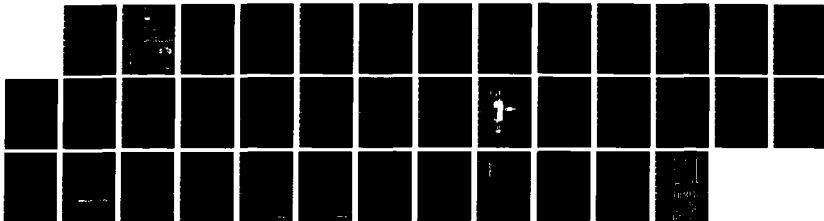
INVESTIGATION OF OPENING SWITCH MECHANISMS BASED ON  
CHEMICALLY REACTIVE PLASMAS(U) GTE LABS INC WALTHAM MA  
W P LAPATOVICH ET AL NOV 85 N00014-82-C-0615

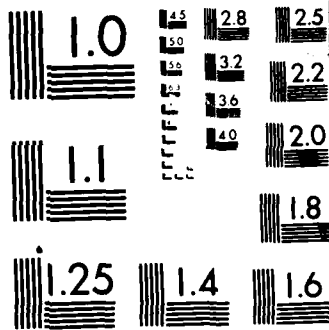
1/1

UNCLASSIFIED

F/G 9/5

NL





MICROCOPY RESOLUTION TEST CHART  
NBS 1963-A

**Research &  
Development**



**AD-A163 171**

**Office of Naval Research  
Contract No. N00014-82-C-0615**

**Final Technical Report  
Investigation of Opening Switch Mechanisms  
Based On Chemically Reactive Plasmas**

by  
**W.P. Lapatovich  
R.B. Piejak  
J.M. Proud**

This document has been approved  
for public release and sale; its  
distribution is unlimited.

**GTE Laboratories Incorporated  
40 Sylvan Road  
Waltham, MA 02254**

**November 1985**

**GTE**

NO 00014-82-C-0615

**OFFICE OF NAVAL RESEARCH  
CONTRACT NO. N00014-82-C-0615**

**FINAL TECHNICAL REPORT  
INVESTIGATION OF OPENING SWITCH MECHANISMS  
BASED ON CHEMICALLY REACTIVE PLASMAS**

by

**W.P. Lapatovich  
R.B. Piejak  
J.M. Proud**

**November 1985**

**GTE Laboratories Incorporated  
Waltham, MA 02254**

**Reproduction in whole or in part is permitted for  
any purpose of the U.S. Government**

**Approved for Public Release; Distribution Unlimited**

AD-A163771

REPORT DOCUMENTATION PAGE		READ INSTRUCTIONS BEFORE COMPLETING FORM
1. REPORT NUMBER N-00014-82-C-(F)	2. GOVT ACCESSION NO. AD-A163771	3. RECIPIENT'S CATALOG NUMBER
4. TITLE (and Subtitle) Investigation of Opening Switch Mechanisms Based on Chemically Reactive Plasmas		5. TYPE OF REPORT & PERIOD COVERED Final Report 15 Aug 1982 30 Oct 1985
		6. PERFORMING ORG. REPORT NUMBER
7. AUTHOR(s) W.P. Lapatovich, R.B. Piejak, J.M. Proud		8. CONTRACT OR GRANT NUMBER(s) N-00014-82-C-0615
9. PERFORMING ORGANIZATION NAME AND ADDRESS GTE Laboratories, Inc. 40 Sylvan Road Waltham, MA 02254		10. PROGRAM ELEMENT, PROJECT, TASK AREA & WORK UNIT NUMBERS
11. CONTROLLING OFFICE NAME AND ADDRESS Office of Naval Research 800 N. Quincy St. Arlington, VA 22217		12. REPORT DATE Nov 1985
		13. NUMBER OF PAGES 30
14. MONITORING AGENCY NAME & ADDRESS (if different from Controlling Office)		15. SECURITY CLASS. (of this report) Unclassified
		15a. DECLASSIFICATION/DOWNGRADING SCHEDULE
16. DISTRIBUTION STATEMENT (of this Report)  Approved for public release; distribution unlimited.		
17. DISTRIBUTION STATEMENT (of the abstract entered in Block 20, if different from Report)		
18. SUPPLEMENTARY NOTES		
19. KEY WORDS (Continue on reverse side if necessary and identify by block number) Chemically Reactive Plasmas, Opening Switches, Transient Plasmas, Pulsed Discharges.		
20. ABSTRACT (Continue on reverse side if necessary and identify by block number) An investigation of discharge-induced chemical reactions resulting in high-density product vapors containing strongly attaching gases has been conducted to evaluate the feasibility and potential of such reactions in rapid opening plasma switches. This new concept of employing such reactions to limit and/or interrupt large currents on a microsecond time scale was studied in two element (electrodeless and electroded) devices and in three element (electroded) devices. Bimolecular and unimolecular reactions were considered. The plasma reaction		

Block #20

between  $AlCl_3$  and  $SiO_2$  was studied. The electrical properties of one of the reaction products ( $SiCl_4$ ) is reported herein.

ABSTRACT

An investigation of discharge-induced chemical reactions resulting in high-density product vapors containing strongly attaching gases has been conducted to evaluate the feasibility and potential of such reactions in rapid opening plasma switches. This new concept of employing such reactions to limit and/or interrupt large currents on a microsecond time scale was studied in two element (electrodeless and electroded) devices and in three element (electroded) devices. Bimolecular and unimolecular reactions were considered. The plasma reaction between  $AlCl_3$  and  $SiO_2$  was studied. The electrical properties of one of the reaction products ( $SiCl_4$ ) is reported herein.

RE: Company Private, For Distribution Within  
GTE Only  
Delete the above statement. The document was  
funded by Office of Naval Research.  
Per Dr. Bobby R. Junker, ONR/Code 1112

Accession For	
NTIS CRA&I	<input checked="" type="checkbox"/>
DTIC TAB	<input type="checkbox"/>
Unannounced	<input type="checkbox"/>
Justification	
By	
Distribution /	
Availability Codes	
Dist	Avail and/or Special
A-1	



## CONTENTS

<u>Section</u>	<u>Page</u>
1 Introduction	1
2 Experimental Results	2
3 Conclusions and Suggestion for Further Work	9
4 References	11
5 Illustrations	13
6 Appendix	19

## ILLUSTRATIONS

<u>Figure</u>	<u>Page</u>
1 Experimental system for three element device	13
2 Photograph of Macor test bed	14
3 Voltage and current measurements on three electrode device	15
4 Experimental Data - no Ablative material in charging path	16
5 Experimental Data - Ablative material is $H_3BO_3$ in this test	17
6 Experimental Data - Ablative material is $AlCl_3$ in this test	18

## Introduction

Inductive energy storage is of interest in pulse power technology because of its relatively high-energy density in comparison with capacitive energy storage systems (1). To operate effectively an inductive storage system requires a repetitive fast opening switch which can conduct current long enough to charge a storage inductor and then become sufficiently resistive to divert the current from the switch to a load. Such a device is of crucial importance in a wide range of applications such as directed energy weapons, discharge lasers, x-ray generators, mass drivers and nuclear weapons simulators (2). The desired opening switch performance has been achieved with varying degrees of success. Electron beam controlled opening switches have perhaps been the most successful (3,4) although other switching concepts based on optically controlled discharges (5), spark gaps (6), thyratrons (7) , and vacuum interruptors (8) are being studied. Highly specialized devices such as the plasma erosion (9) switch have also exhibited the desired switching characteristics.

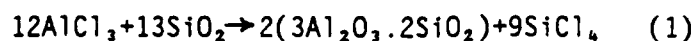
Our research has concentrated on exploring yet another concept to produce current diversion required in an opening switch. Specifically, our approach relies on an in situ chemical modification of the plasma conductivity. It is well known that during a discharge various molecular species with markedly different electrical properties from their precursors can be formed. If properly chosen, these discharge products can alter the plasma conductivity and cause current interruption. This concept is appealing because of its simplicity, requiring no external energy source to control the switching function. Activation is due to joule heating in the discharge and occurs when energy deposition exceeds a threshold level.

Our initial concept for a fast opening switch consisted of a two electrode device operating at an elevated temperature (150°C) in a gaseous environment of a vaporized solid (metal halide). Bimolecular reactions between the metal halide and another species yielding products with the desired electrical properties were investigated as a promising switching medium. As our experiments progressed, we refined our concepts and shifted our focus to unimolecular reactions and three electrode experimental devices. The results of our experiments, conclusions, and suggestions for additional work are detailed in the following sections.

### Experimental Results

Our best results have been obtained in a three electrode device. A third electrode was added to the initial device because we found that an alternative current path was needed to prevent restrike in the charging path. In this device a solid phase material is the initial reactant. The apparatus is operated at room temperature and the ablation of the solid provides the reactant gas. Unimolecular reactions, i.e. dissociation of the reactant gas into attaching fragments, are preferred over the slower bimolecular reactions initially sought. During current diversion the active electron loss mechanisms are attachment to the reactant gas and its fragments and  $J \times B$  forces directing the discharge into the walls of the apparatus. At the same time  $E/N$  decreases due to an increase in  $N$  (gas density) and leads to a decrease in electron production since the ionization rate is a sensitive function of  $E/N$ . Before discussing in detail the circuit, apparatus, and the results of these experiments, we will give a brief synopsis of our earlier experimental efforts and their gradual maturation into our present current diverting device.

The objective of the first series of experiments was to confirm the bimolecular reaction that we had postulated would occur in a plasma discharge. Specifically, the reaction between metal halide molecules and vitreous silica ( $\text{SiO}_2$ ) was believed to create an inert precipitate and a volatile electron attaching gas. Aluminum trichloride vapor ( $\text{AlCl}_3$ ) was confined in an ultra-clean vitreous silica vessel and an electrodeless rf discharge was initiated. The predicted reaction



was found to occur. This was established through spectroscopic observation of discharge fragments ( $\text{Al}$ ,  $\text{SiCl}$ ,  $\text{AlCl}$ , etc.), and, through post mortem examination of the inner surface of the discharge chamber (Auger spectroscopy) and the gas in the discharge vessel (GC mass spectroscopy). Indeed all the  $\text{AlCl}_3$  was consumed in the discharge leading to chemical vapor deposition of an aluminosilicate film on the inner surface of the discharge tube. In addition,  $\text{SiCl}_4$ , a good electron attacher, was formed in the gas phase. The reaction was fast, the rf discharge duration being but a fraction of a second. After this it was impossible to sustain the discharge with our apparatus because the atmosphere in the discharge vessel had been irreversibly modified by the creation of  $\text{SiCl}_4$ . The increased gas breakdown voltage after the reaction suggested a possible mechanism for real time current interruption due to changes in the electrical characteristics of the gas fill. The present geometry precluded the implementation of non-invasive diagnostics forcing us to reconfigure the experiments. (See Appendix 1 for a more detailed discussion of the electrical properties of  $\text{SiCl}_4$  and experiments supporting this work.)

In the next series of experiments we studied the effect of the bimolecular reaction on current flow and the possibility of current limiting or interruption brought upon by the bimolecular reaction. The discharge vessels (5mm ID tubing) had two electrodes (anode and cathode), and contained solid  $\text{AlCl}_3$  in a buffer gas at a pressure of a few Torr. The discharge tubes were immersed in a constant temperature oil bath ( $T < 130^\circ\text{C}$ ) to raise the vapor pressure of the  $\text{AlCl}_3$  to a few Torr. The oil was transparent to visible and soft UV radiation. The optical emission from the discharge was monitored with a monochromator and a fast photomultiplier (2ns risetime).

In the first series of tests the discharge tubes were pyrex and the current source was a 0.5 ohm pulse forming network (pfn) with a 10  $\mu\text{s}$  duration. Temporally resolved Al emission at 394 nm and  $\text{AlCl}$  emission at 527 nm were monitored along with discharge current and voltage. A peak current density of  $20\text{kA}/\text{cm}^2$  with a peak energy density of  $70\text{ J}/\text{cm}^3$  was observed. The temporal evolution of Al and  $\text{AlCl}$  emission followed the current wave shape suggesting that the anticipated reaction did occur but no current limiting or interruption was observed. The breakdown voltage of the discharge tube doubled after the initial discharge in tubes containing  $\text{AlCl}_3$  and  $\text{SiO}_2$ .

Because of the high energy density in these experiments we believed that the  $\text{SiCl}_4$  may have fragmented. The experiments were therefore repeated with a new pfn (81 ohms) and quartz discharge tubes. The new pfn reduced the energy dissipated in the discharge by a factor of 100 thus reducing the fragmentation of the discharge products. The quartz discharge tubes allowed us to observe shorter wavelength emission from the discharge. In these experiments the Al line at 309 nm and the  $\text{SiCl}$  molecular bands at 288 nm were monitored. Again, the time variation of the emission from both species followed the discharge

current but neither current limiting nor interruption was observed. Based on these observations and a calculation of the reactant mixing rates we concluded that although vapor phase bimolecular reactions are fast (<100 ns), the mixing of gaseous  $\text{AlCl}_3$  and solid  $\text{SiO}_2$  is slow (100's of  $\mu\text{s}$ ). Consequently, the concentration of attaching gas from the reaction of  $\text{AlCl}_3 + \text{SiO}_2$  increased too slowly to affect the flow of current through the discharge (a few  $\mu\text{s}$ )

Unimolecular reactions offer the possibility of producing a copious amount of reaction product in very short times ( $\mu\text{s}$ ) In this series of experiments we focussed on creating a discharge in which the current could be limited or interrupted by a unimolecular reaction (ablation). A surface discharge was chosen to provide enough radiant flux to ablate the reactant surface. The ablation rate (10),  $v_{ss}$  is given by:

$$v_{ss} = F / \rho \{L + c(T_v - T_0)\} \quad (2)$$

where:  $F$  is the radiant intensity in  $\text{W}/\text{cm}^2$ ,  $L$  is the specific heat of vaporization per unit mass,  $\rho$  is the density,  $c$  is the heat capacity per unit mass,  $T_0$  is the initial temperature of the material and  $T_v$  is the vaporization temperature. For carbon  $L=171$  kcal/gram-atom,  $\rho=2.26$  g/cm<sup>3</sup>,  $c=0.165$  cal/g/°C, and  $T_v=4830^\circ\text{C}$ . For this case, a radiant flux of  $10^6$   $\text{W}/\text{cm}^2$  would produce an ablation rate ( $v_{ss}$ ) of 550cm/s. A ten  $\mu\text{s}$  discharge with that radiant flux would ablate  $7.5 \times 10^{20}$  atoms from the surface. The dissociation of the ablated material (hydrocarbon or flouorocarbon based plastic was used instead of carbon) served the dual purpose of decreasing the  $E/N$ , and providing electron attaching fragments.

The evolution of the spectrally integrated light from surface discharges was observed with a PIN photodiode (2ns response). The surface discharges

were produced in a gap (1mm x 10mm) in a stripline transmission system. For discharges open to the atmosphere, the light output followed the current. For discharges confined within mylar dielectric of a stripline gap, the light output exhibited anomalous behavior; i.e., the light output peaked when the current was at a minimum (but not zero). Spectrally resolved emission, integrated over the current pulse duration, was also recorded using parallel detection technology (gated, intensified vidicon-PARC OMAII, Princeton, N.J.) For a discharge confined in mylar dielectric, the emission spectrum (largely continuum) was fitted to a blackbody at  $T=3500^{\circ}\text{K}$  (assuming unit emissivity). At this temperature the plasma does not produce enough radiant density to ablate the substrate material. Radiant flux from a blackbody at  $3500^{\circ}\text{K}$  is  $850\text{ W/cm}^2$ . This is about four orders of magnitude lower than required for substantive ablation due to radiation. In principle, the plasma should achieve a much higher radiant intensity if losses in the stripline are neglected. The expected maximum energy density has been calculated and is  $6 \times 10^7\text{ W/cm}^2$ . Losses in the stripline and less than unit emissivity prevent attainment of this high radiant flux. However, surface damage was observed, presumably due to thermal (or contact) ablation. Although current interruption was not observed in these experiments the large  $di/dt$  caused by the rapid changes in plasma impedance due to ablation resulted in restrike and current flow at reduced levels. The recurring restrike problem led us to reconsider the experimental design and modify the apparatus.

Keeping with the ablation concept, in the present device a third electrode has been added to the previous configuration to provide both a charging current path and a load current path. A schematic diagram of the three element device and the external circuit is shown in Figure 1. A 5 kV dc supply

charges a 10  $\mu\text{F}$  capacitor bank. An externally triggered HV pulser synchronized with the detection electronics provides a trigger pulse to the spark gap. When the spark gap fires, the capacitor bank discharges and current flows from the source electrode (1) to the charging electrode (2) through about 100 ohms to ground (charging current path). This current flow charges the inductor (0.675  $\mu\text{H}$ ) connected to the source electrode. The background pressure in the device and the separation between the source electrode and the load electrode (3) determine the duration of the charging current. After charging the inductor, the main current path breaks down and current is diverted from the charging circuit and flows from the source to the load electrode. The pd (pressure x distance) of the load current path is set so that it cannot break down unless the charge current path does so first. The HV diode connecting the load and charging path encourages current interruption in the charging path.

A photograph showing the present three element device is shown in Figure 2. The electrode on the right is the source electrode, the center electrode is the charging electrode and the electrode on the left is the load electrode. The device is made of machineable ceramic (MACOR) and is extremely durable. Easily vaporizable material is inserted into the charging path to aid in the current interruption by increasing the gas density and creating attachers. The materials tested were: aluminum trichloride ( $\text{AlCl}_3$ ), orthoboric acid ( $\text{H}_3\text{BO}_3$ ) and copper carbonate dihydroxide ( $\text{CuCO}_3(\text{OH})_2$ ). The gas pressure in the device is controlled by a vacuum pump and monitored with a mechanical vacuum gauge. Tests have been done between 50 and 120 Torr of room air. The pressure partially controls the duration of the charging current pulse.

A diagram showing the diagnostics used to monitor the tests is shown in Figure 3. The differential voltage between the source and charging electrode

and the voltage across the load resistor are measured with Tektronix 6015 high voltage probes and stored in a Biomation 8100 waveform recorder. In this way the charge path voltage and load current are monitored. A Pearson (Model 110) current probe is used to measure the charging current. Load currents of 5 or 6 kA are typical; the charging current is between 25 and 30 amps. The voltage across the charging path varies with the ablating material in the charge path.

About 70 different tests were conducted under various conditions of gas pressure, ablative materials and electrode separations. Representative data is shown in Figures 4,5 and 6. Measurements taken with no ablater in the charge path are shown in Figure 4. The top graph shows a charging current of about 30 amps flowing before the main gap breaks down and only a few amps thereafter. This curve serves as a reference showing the charging current when no ablation occurs. The middle graph is the voltage across the charging path. The voltage across the charging path is very small because there is no ablation. The lower graph is the main discharge current and is virtually identical in Figures 4,5 and 6 because the current in the main discharge path is not affected by the ablation in the charging path. The same measurements are shown in Figure 5; however, in this test boric acid was inserted into the charging path. In the charging current plot, current limiting is observed due to the ablation of the boric acid. Ideally, if enough material is ablated, the charging current will cease at the instant the main gap current begins to flow. In the middle plot there is a large increase in charge path voltage due to the ablater. Because the charge voltage increases the charging current decreases. The lower trace is about same as in Figure 4. Finally, similar measurements were recorded in  $AlCl_3$ . The effect for  $AlCl_3$  (see Figure 6) is not as large as that observed in  $H_3BO_3$ . This result was difficult to obtain

because the  $AlCl_3$  would deliquesce in the presence of room moisture altering the chemical and physical properties of the compound. Special precautions were taken to keep this material as dry as possible for this test.

#### Conclusions and Suggestions for Further Work

The final experiments indicate that current limiting can be attained through a combination of ablation and attachment. Clearly the device is not optimized for switching purposes but designed so the ablative effects could be observed. Changes in the parameters of the experiment are necessary to determine if this scheme can bring on total current interruption. Specifically the resistance in the charge path should be reduced (or even eliminated) and the resistance in the load path should be increased. This would permit a higher charge current resulting in more energy stored in the inductor and consequently increased ablation. These conditions would favor a decrease of  $E/N$  and an increase in attaching gas, thereby increasing the likelihood of current interruption. Reducing the load path resistance would also increase the amount of stored energy diverted into the load. Another avenue to explore would involve increasing the voltage and current levels in this device to more practical levels. In our experiments we limited the high voltage to 5 kV which was adequate to demonstrate the desired effect, namely interruption of current flow through chemical modification of the discharge species (via dissociation).

Improvements in the performance of this device can be anticipated with further work. The device was designed to test the concept and in a single shot mode it worked well. Practical opening switches require repetitive operation and improvements in this area are necessary. We could envision switching de-

vices (based on chemical modification of the plasma constituents) with dimensions larger than can be comfortably housed in a typical laboratory. These devices might employ Roots blowers to exchange the discharge atmosphere after each shot - a concept which would support repetitive switch action. Additionally, novel methods for introducing the chemical reactants might be explored. For example, a mixture of granulated  $\text{SiO}_2$  and  $\text{AlCl}_3$  might be entrained in the dilute but rapid flow of background gas (e.g. rare gases) in a flowing system. Such a system also presents the potential for a quasi-closed cycle where the inert gas would be scrubbed and recycled while the volatiles are condensed out of the system. In this case, the only consumable would be the solid, granular reactants.

## REFERENCES

1. J.K. Burton, D. Conte, R.D. Ford, W.H. Lypton, V.E. Scherrer and I.M. Vitkovitsky " Inductive Storage - Prospects for High Power Generation," Proc. 2nd IEEE Int. Pulsed Power Conf., Lubbock, TX, 1979, pg. 284.
2. M.F. Rose, A.K. Hyder, Jr., "Workshop on Diffuse Discharge Opening Switches," January 1982, Tamarron, Co. M. Kristiansen, K.H. Schoenbach Eds.
3. R.J. Comisso, R.F. Fernsler, V.E. Scherrer and I.M. Vitkovitsky "High Power Electron-beam Controlled Switches," November 1984, Rev. Sci. Instruments, Vol. 55 (11), p. 1834.
4. P. Bletzinger, Proceedings of the 4th IEEE Pulse Power Conference, Albuquerque, NM, 1983, p. 37.
5. K.H. Schoenbach, G. Schaffer, M. Kristiansen, L.L. Hatfield, and A.H. Guenther, "Concepts for Optical Control of Diffuse Discharge Opening Switches," IEEE Trans. on Plasma Science, Vol. PS-10, No. 4, December 1982, p. 246.
6. C.H. Yeh, M. Hagler, and M. Kristiansen, "Voltage Recovery Measurements in a High Energy Spark Gap," 4th IEEE Pulse Power Conference, Albuquerque, NM, 1983, p. 159.
7. M. Gunderson, J.A. Kunc, D. Erwin, and C. Braun, Fundamental Processing in High Current Glow Discharge Switches, 5th IEEE Pulse Power Conference, June 1985, Session 3-5.
8. F.T. Warren, J.M. Wilson, J.E. Thompson, R.L. Boxman, and T.S. Sudarshan, "Vacuum Switch Trigger Delay Characteristics," IEEE Trans. on Plasma Science, Vol. PS-10, No. 4, December 1982, p. 298.

9. P.F. Ottinger, S.A. Goldstein, R.A. Meger, "Theoretical Modeling of the Plasma Erosion Opening Switch for Inductive Storage Applications," J. Appl. Phys., 56 (3), August 1984, p. 774.
10. J.F. Ready, "Effects of High Power Laser Radiation," Academic Press, New York, NY, (1971), Ch. 3, Section D.

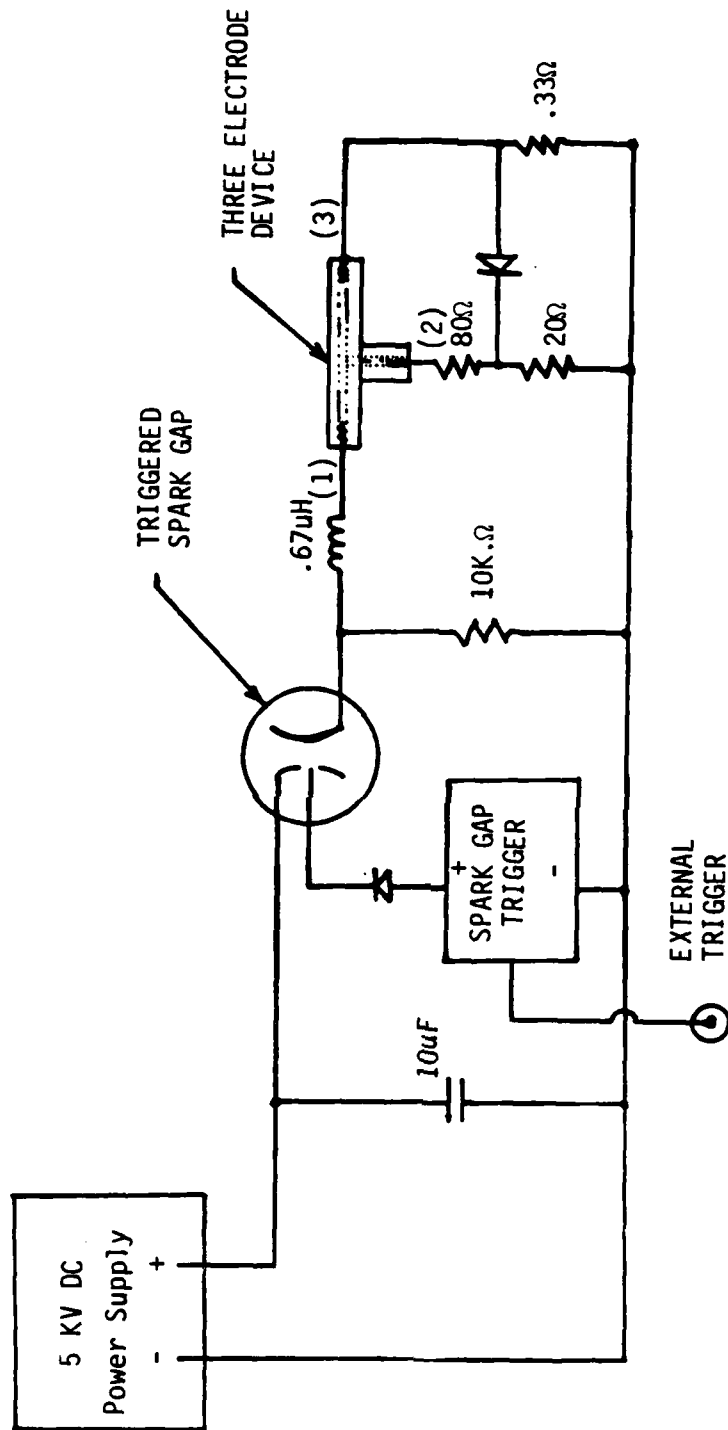


Figure 1. Experimental system for three element device.

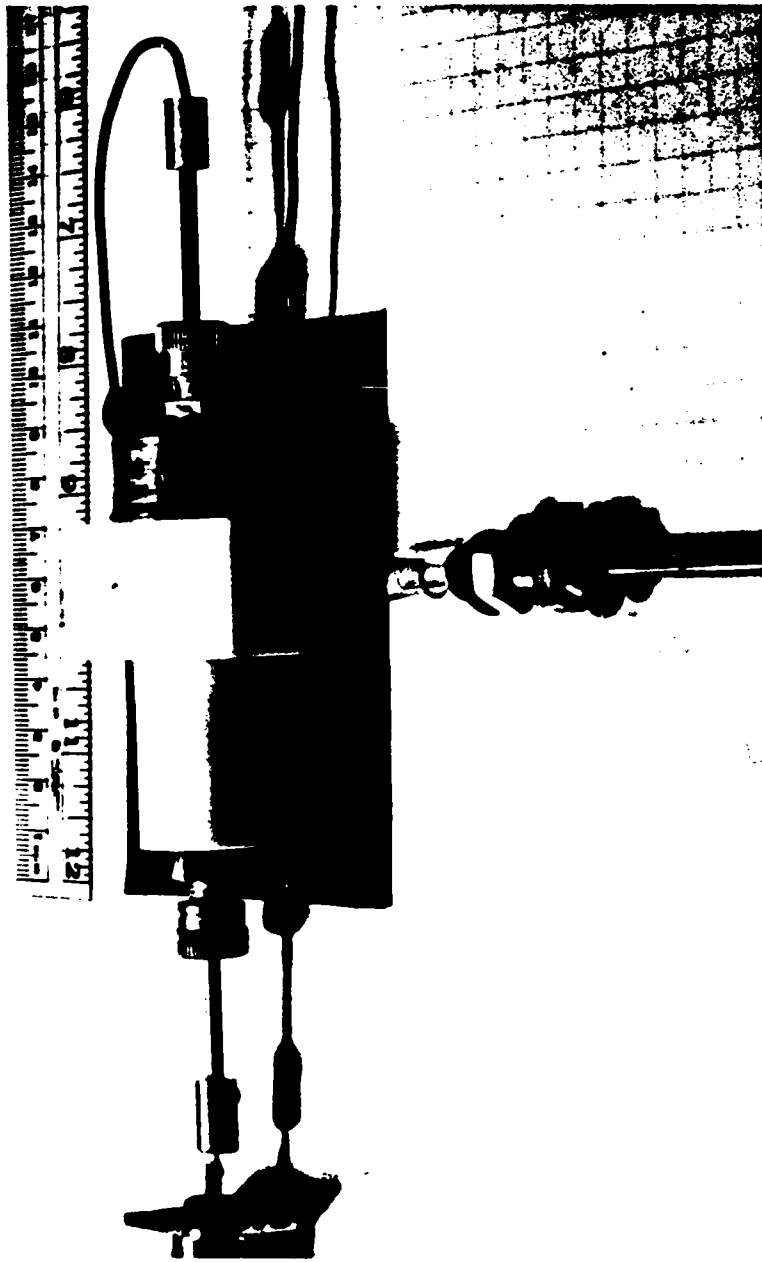


Figure 2. Photograph of Macor test bed. The charge path is vertically oriented in this picture. The load path is horizontal.

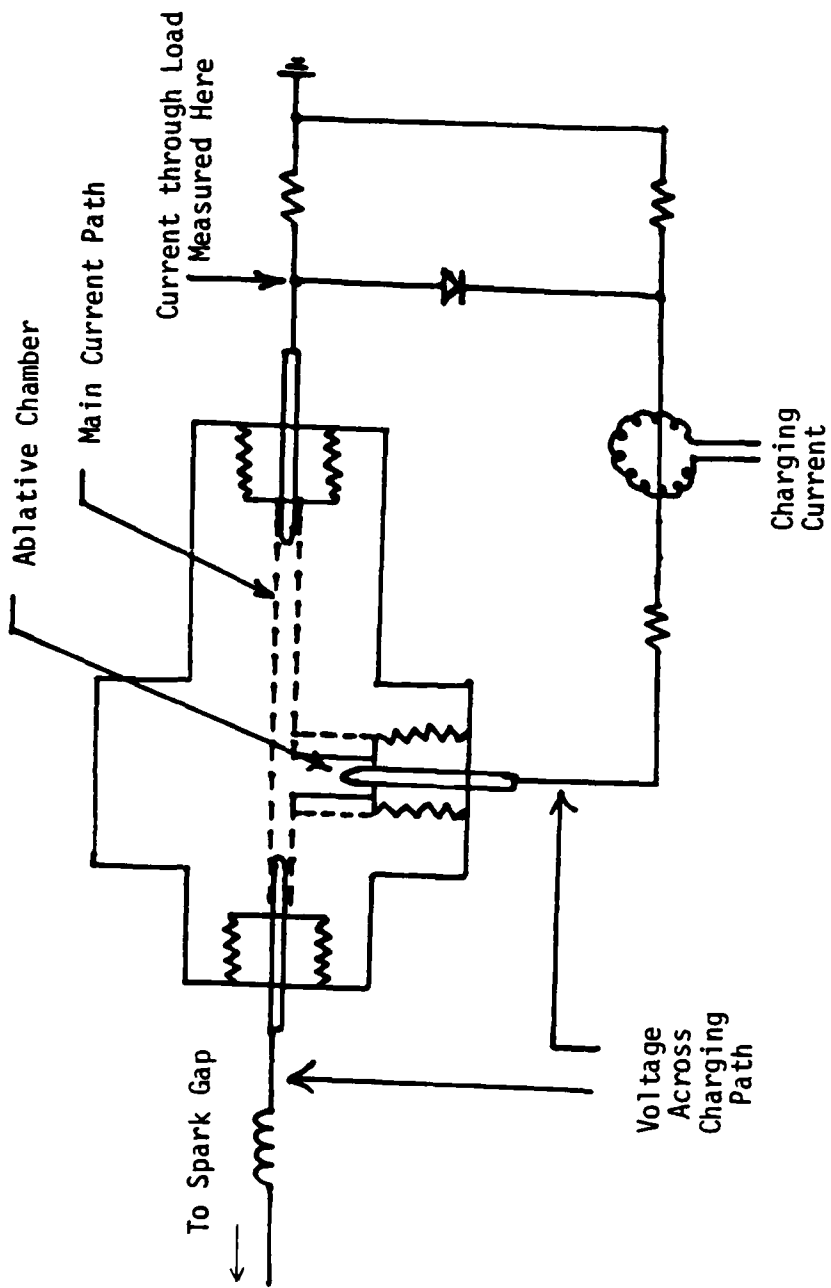


Figure 3. Voltage and current measurements on three electrode device.

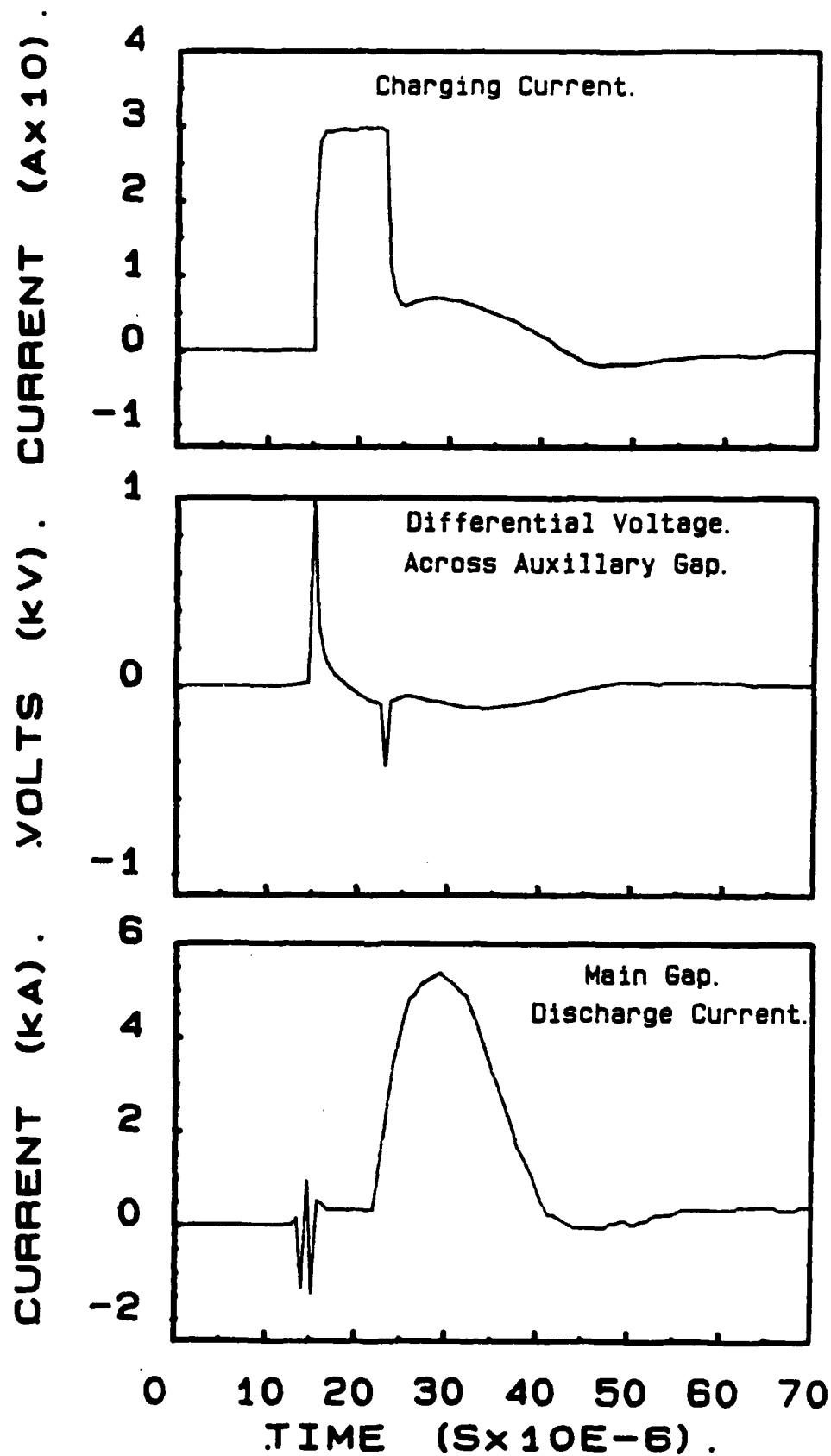


Figure 4. No ablative material in charging path.

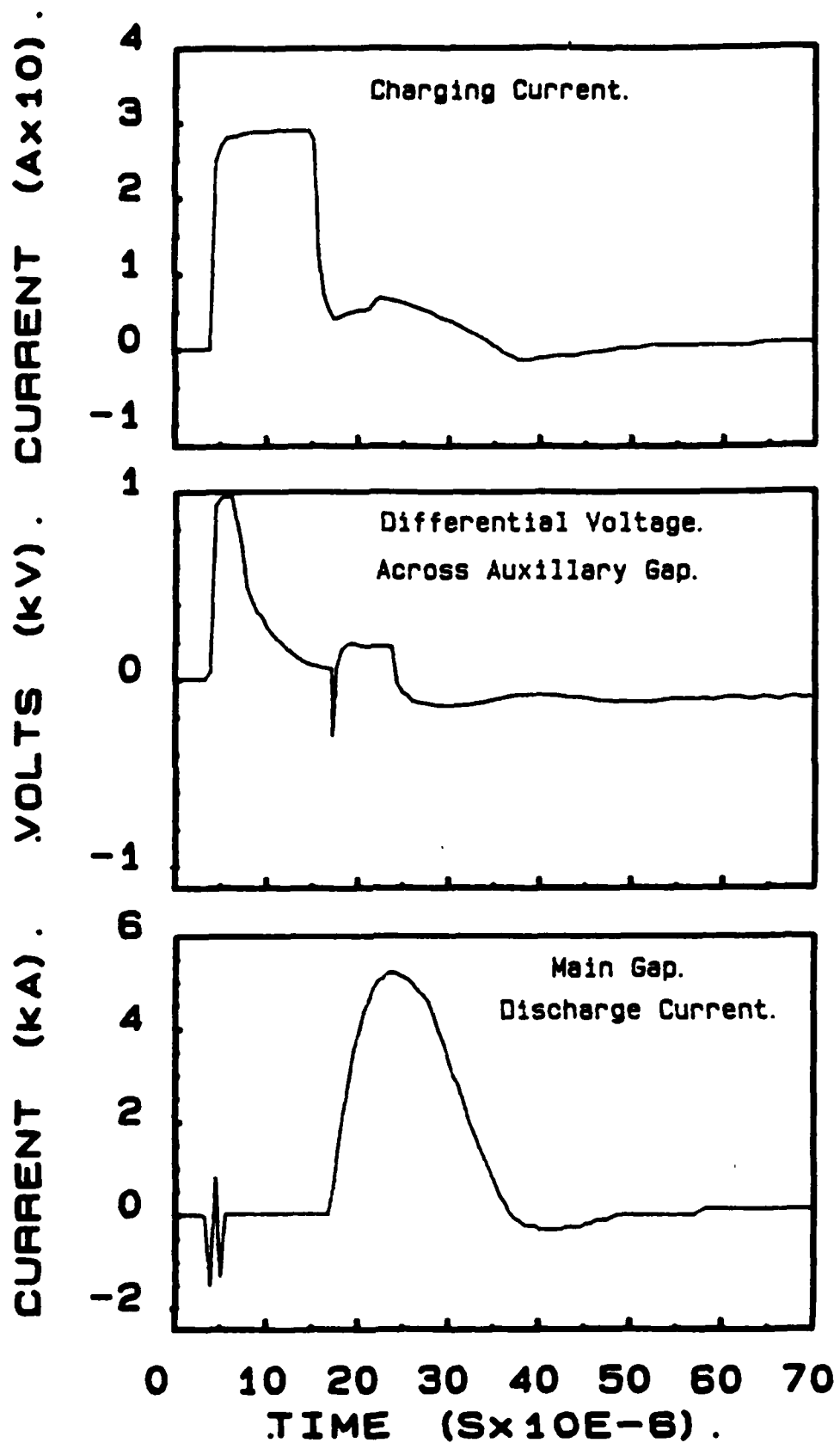


Figure 5. The ablative material was  $H_3BO_3$  in this test.

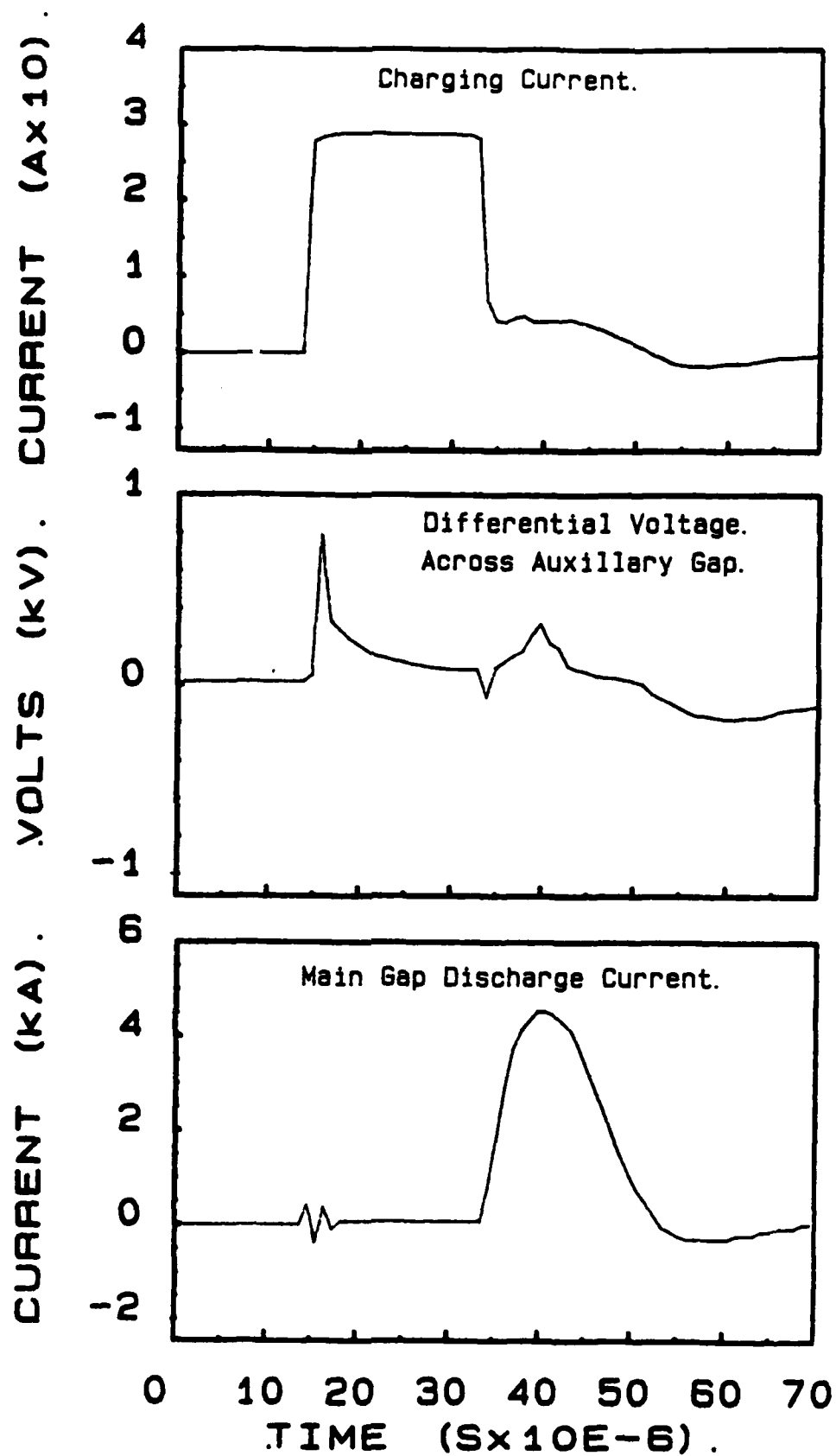


Figure 6. The ablative material was  $AlCl_3$  in this test.

## APPENDIX

1. "Measurements of Effective Ionization Rates in Transient Gas Discharges" - IEEE International Conference on Plasma Science, San Diego, CA, May 23-25, 1983.
2. "E/N in Transient Gas Discharges" - 4th IEEE Pulsed Power Conference, Albuquerque, NM, June 6-8, 1983.
3. "Transient Gas Discharges in Perfluorocarbons" - Conference on Electrical Insulation and Dielectric Phenomena, Buck Hill Falls, PA, October 16-20, 1983.
4. "Formation and Decay of Nanosecond Discharges in Electron Attaching Gases" - 36th Annual Gaseous Electronics Conference, Albany, NY, October 11-14, 1983.
5. "Net Ionization Rates in Electronegative Gases" - 4th International Symposium on Gaseous Dielectrics, Knoxville, TN, April 29 - May 3, 1984.

MEASUREMENTS OF EFFECTIVE IONIZATION RATES  
IN TRANSIENT GAS DISCHARGES

by

W.W. Bysszewski, M.J. Enright, J.M. Proud  
GTE Laboratories

For many molecular gases, vapors and their mixtures, there are no available data for drift velocity, ionization and attachment coefficients, nor for dielectric strength. Studies of transient gas discharges can provide a partial data base. In particular, such studies offer two techniques for the determination of the net ionization rate for a range of  $E/N$  values above the static breakdown limit,  $(E/N)_{dc}$ .

The first, based on investigations of formative times in short, overvolted pulse discharges, can map the net ionization collision frequency over a range in which  $(E/N) > (E/N)_{dc}$ . In practice, the effective ionization rate is inversely proportional to the formative time. The coefficient of proportionality depends only slightly on the initial electron density. The accuracy of this technique depends largely on the accuracy with which this coefficient can be determined.

The second technique is based on analysis of the leading edge of the transmitted current waveform. As the current through the gas rises, the voltage across it drops because of the finite impedance of the external circuit. This causes a continuous change of  $E/N$  in the gap. The reduced field changes from the applied value  $E_0/N$  to a final value  $(E/N) = (E/N)_{dc}$  at which the effective electron growth rate equals zero. For a gas whose drift velocity depends linearly on  $E/N$ , it can be shown that the effective ionization collision frequency at a given moment is directly proportional to the time derivative of the current waveform at that moment and inversely dependent on the corresponding current value. Since the current, its derivative and the corresponding value of  $E/N$  can be determined at each point of the current waveform, one can obtain the dependence of effective ionization rate on  $E/N$  for the whole range  $(E/N)_{dc} < (E/N) < (E_0/N)$ . The very fast current rise produced by highly overvolted conditions limits this technique from both a fundamental point of view (equilibrium between electron energy distribution and applied electrical field), and an experimental point of view (time resolution of diagnostic system). This technique may, therefore, be applied in ranges of  $E/N$  representing moderate overvoltages which typically lead to slower current rises.

Experimental investigations performed in a pulse transmission line system<sup>(1)</sup> will be presented. Effective ionization rates in nitrogen and  $SF_6$  determined by means of both techniques will be compared with rates calculated on the basis of published data for drift velocity, ionization and attachment coefficient. This work was partially supported by the Office of Naval Research.

---

1. W.W. Bysszewski, M.J. Enright, J.M. Proud, IEEE Trans. Plasma Sci., PS-10, p. 281 (1982).

## E/N IN TRANSIENT GAS DISCHARGES

W. W. Byszewski, M. J. Enright, J. M. Proud  
GTE Laboratories Incorporated  
Waltham, Massachusetts 02254

### SUMMARY

Current and voltage waveforms in transient gas discharges have been analyzed. A pulse transmission line system was employed to overvolt a test gap filled with various electron attaching gases. The reduced electrical field measured at the zero current growth portion of the discharge was found to be slightly lower than dc or ac breakdown fields for most of the gases studied. The transient discharge technique was also found useful in the determination of plasma resistance during the initial stage of constant current, the phase most likely to exhibit diffuse glow discharge character.

### INTRODUCTION

Processes which occur during the formation of highly overvolted electrical discharges in molecular gases effect the gases' electrical properties. The reduced field at the zero current growth level in transient discharges in attaching gases differs, for instance, from that predicted for the unperturbed gas. It may affect the electron temperature and tend to decrease the plasma resistance. This difference, though typically not large, may become important in the application of transient discharges to pumping gas lasers and to fast switching techniques.

In this paper we present transient current waveforms for several attaching gases ( $\text{SF}_6$ ,  $\text{O}_2$ ,  $\text{CCl}_2\text{F}_2$ ,  $\text{CClF}_3$ ,  $\text{CF}_4$ ,  $\text{CCl}_4$ ,  $\text{SiCl}_4$ ) obtained under a variety of initial conditions. We have measured the reduced field value  $(E/N)_s$ , at which the current growth

reaches zero. This field strength is then compared with the reduced dc breakdown field strength  $(E/N)_{dc}$ , and with the field at which the electron collisional ionization rate is balanced by the electron attachment rate  $(E/N)_c$ . Finally, we analyze the plasma resistance measured during the period of zero current growth, the phase which is most likely to have diffuse glow discharge character.

### EXPERIMENT

The experimental setup used in our investigations of fast breakdown under highly overvolted conditions is shown schematically in Figure 1. A 50 $\Omega$  transmission line system delivers a 45 ns wide, almost rectangular pulse of 20 kV to 30 kV amplitude to the test gap. Gap spacing may be varied from 0.25 cm to 1.75 cm between 4.4 cm dia. plane parallel stainless steel electrodes. Gas pressures have ranged from 30 torr to 1 atm, though most of the data for  $\text{CCl}_4$  and  $\text{SiCl}_4$  vapors have been taken only at the pressures of 30 torr and of 80 torr, respectively. These pressures correspond to the vapor pressures in equilibrium with the liquid phase at 0°C. The test chamber was pumped to  $10^{-2}$  torr before backfilling with the gas to be studied. The chamber was refilled after each series of approximately 10 to 20 discharges.

The statistical breakdown lag time was minimized by initial electrons provided by means of a pulsed UV light source. Current waveforms were monitored with a capacitive divider and recorded by means of a fast transient digitizer. Subnanosecond time resolution and a high level of reproducibility have been achieved.

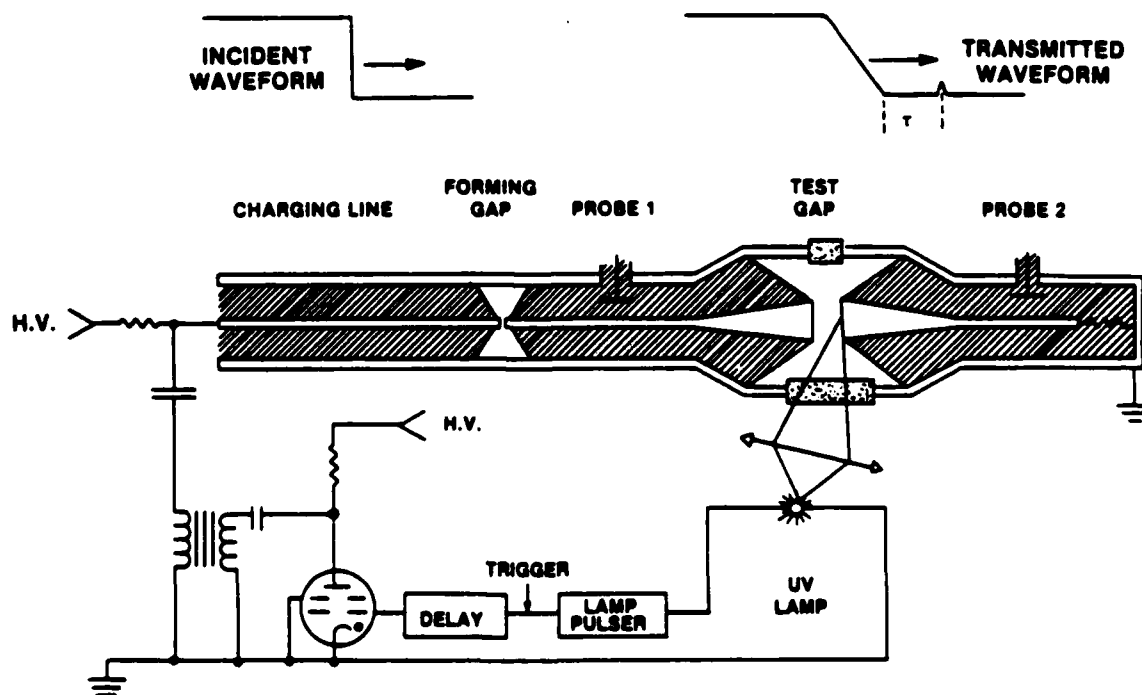


Figure 1. Schematic diagram of the pulsed transmission line system. The circuit synchronizes a UV flash lamp and the forming gap which launches the test pulse.

RESULTS

Current waveforms obtained in SF<sub>6</sub> at two different pressures are shown in Figure 2. Discharge currents, following a formative period, rise rapidly to the value I<sub>s</sub>, at which the total electron production rate is balanced by the electron loss rate. The current remains at this constant level for a time which varies with pressure. The value of reduced field strength, (E/N)<sub>s</sub>, at the current level I<sub>s</sub> may be obtained from the circuit equation for the transmission line system:<sup>1</sup>

$$(E/N)_s = E_0/N - 2Z I_s/dN \quad (1)$$

where:

E<sub>0</sub> = V<sub>0</sub>/d is the applied voltage waveform V<sub>0</sub>(t), divided by the electrode separation, d;

V<sub>0</sub>(t) is represented in current units in Figure 2 and is labeled V<sub>0</sub>/2Z;

Z is the transmission line impedance; and

N is the molecular number density.

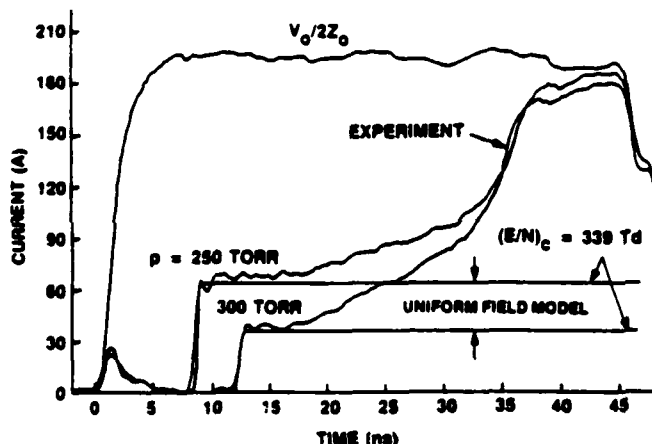


Figure 2. Current waveforms in SF<sub>6</sub> at p=250 torr and p=300 torr; electrode separation d=0.5 cm and amplitude of applied voltage V<sub>0</sub>=20 kV. The incident voltage waveform represented in current units is labeled V<sub>0</sub>/2Z. Numerical results are labeled "Uniform Field Model."

During early phases of the discharge, characterized by the persistent value (E/N)<sub>s</sub>, diffuse glow discharges have been observed in a number of gases.<sup>2-5</sup> The data reported here for SF<sub>6</sub> appear to be consistent with these results. Good agreement between experimentally determined values of I<sub>s</sub> and those calculated on the basis of a uniform field discharge model<sup>1</sup> has been observed as illustrated in Figure 2. This indicates that the field may indeed be uniform and diffuse glow discharge conditions may prevail during this phase. Similar conclusions may be reached through the analysis of current waveforms measured in other electronegative gases. Some typical results are presented in Figures 3 through 6.

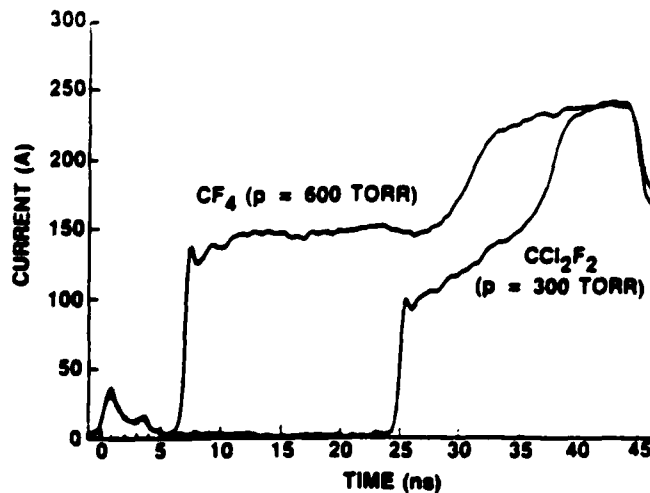


Figure 3. Current waveforms in CF<sub>4</sub> (p=600 torr) and CCl<sub>2</sub>F<sub>2</sub> (p=300 torr). V<sub>0</sub>=25 kV, and d=0.5 cm.

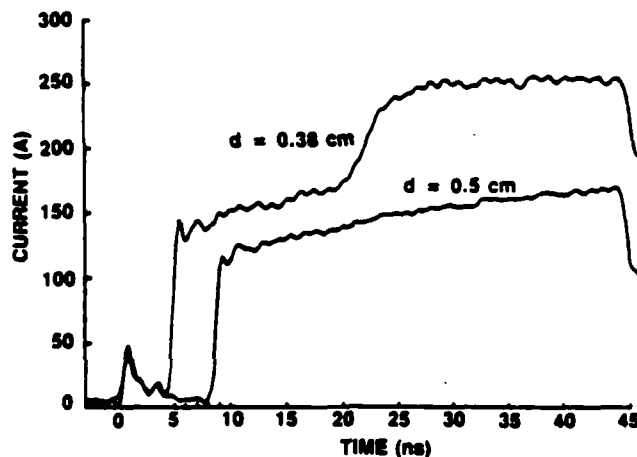


Figure 4. Current waveforms in CClF<sub>3</sub> (Freon 13) at d=0.38 cm and d=0.5 cm, pressure p=500 torr and V<sub>0</sub>=25 kV.

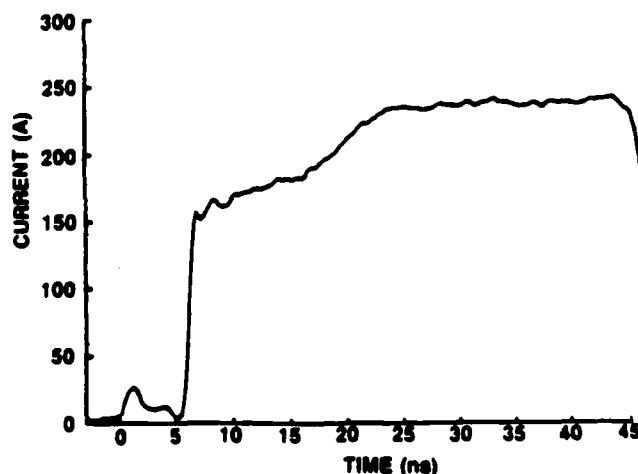


Figure 5. Current waveform in SiCl<sub>4</sub> at a cold spot temperature T=0°C (p=80 torr), d=0.75 cm and V<sub>0</sub>=25 kV.

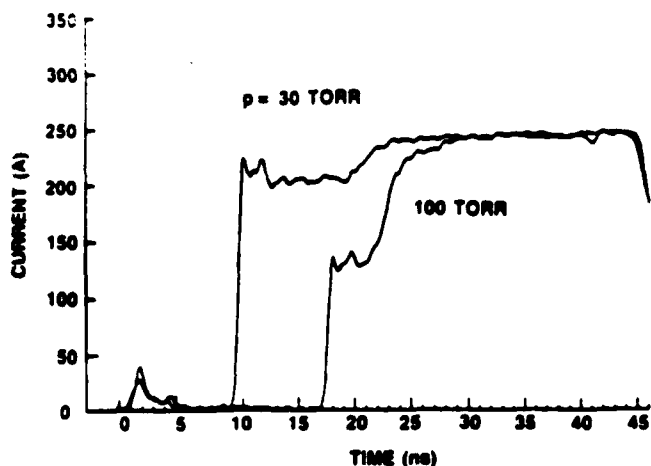


Figure 6. Current waveforms in  $\text{CCl}_4$  at cold spot temperature  $T=0^\circ\text{C}$  ( $p=30$  torr) and  $T=23^\circ\text{C}$  ( $p=100$  torr),  $d=0.5$  cm and  $V_0=25$  kV.

The constant current portion of the discharge is followed by a gradual increase in current and a subsequent steep rise to a value limited by the impedance of the external circuit. In the final stage of the discharge, the plasma resistance reaches low values characteristic of arc conditions. The current rise from  $I_s$  to the circuit limited value therefore represents a transition from glow to arc discharge conditions.<sup>2-6</sup> It is noteworthy that such a clear illustration of this transition in electronegative gases on a nanosecond time scale as shown in Figures 2 through 6 seems to be rather unique and to the best of our knowledge has been demonstrated previously only in  $\text{SF}_6$ .<sup>5,6</sup> In contrast, the current observed in non-attaching nitrogen is seen to rise, in our experiment, smoothly towards the circuit limited value.<sup>1</sup>

In Figure 3 current waveforms in  $\text{CCl}_2\text{F}_2$  (Freon 12) and  $\text{CF}_4$  (Freon 14) are compared.  $\text{CCl}_2\text{F}_2$ , a much stronger attacher, has an  $(E/N)_s$  value higher than that of  $\text{CF}_4$ . This can be readily seen from Figure 3, where comparable values of  $I_s$  have been reached even though the incident reduced fields differ by a factor of two. Since all the gases studied do not have an appreciable flat section of the current waveform (e.g.,  $\text{CCl}_2\text{F}_2$  in Figure 3),  $I_s$  has been taken experimentally as the average between the first maximum and minimum of the current waveform after breakdown. This represents the first point at which current growth equals zero and is a feature found in all cases of interest. Although the flat section of the  $\text{CF}_4$  waveform lies slightly above this value, glow conditions may still prevail for this region.

A long gradual current rise from  $I_s$  is observed in  $\text{CClF}_3$  (Freon 13), as shown in Figure 4. Here waveforms taken at two different electrode separations,  $d = 0.5$  cm and  $d = 0.38$  cm, are presented. In the case with a lower initial field ( $d = 0.5$  cm), the full transition to an arc stage does not occur within the 45 ns pulse width.

A current waveform in silicon tetrachloride ( $\text{SiCl}_4$ ) vapor at a cold spot temperature of  $0^\circ\text{C}$  ( $p = 80$  torr) is shown in Figure 5. The incident reduced field for measurements in  $\text{SiCl}_4$  was controlled by the electrode separation and the amplitude of the applied voltage only. Although  $\text{SiCl}_4$  has a high

dielectric strength, it exhibits a rather slow glow-to-arc transition.

Typical current waveforms in carbon tetrachloride ( $\text{CCl}_4$ ) at two cold spot temperatures,  $0^\circ\text{C}$  and  $23^\circ\text{C}$  ( $p = 30$  torr and  $100$  torr), are compared in Figure 6.  $\text{CCl}_4$  has the highest dielectric strength of the compounds studied and displays a very rapid current rise to  $I_s$ . The current then falls slightly from  $I_s$  to a flat portion probably representing a glow stage. The flat portion of the current waveform appearing at a value lower than  $I_s$  may be due to transient non-equilibrium conditions in the discharge.

## DISCUSSION

Current waveforms such as those illustrated in Figures 2 through 6 were used to provide values of  $I_s$  from which  $(E/N)_s$  could be calculated with Eq (1). The results summarized in Table 1 were derived from repeated experiments representing, typically, 25 different combinations of the initial parameters  $V_0$ ,  $d$  and  $N$  to yield an average value and the standard deviation as tabulated. The standard deviations do not include the uncertainties in the measurement of  $I_s$ . The wavy character of the current waveforms at this point is related to the rapid decrease in the net ionization rate to zero when the field collapses from a highly overvolted state to the breakdown value, and provides the main source of error in individual  $I_s$  determinations.

TABLE 1  
REDUCED FIELD AT BREAKDOWN FOR  
VARIOUS GASES AND VAPORS

Gas/ Vapor	$(E/N)_s$ (Td)	$E_0/N$ (Td)	$(E/N)_c$ (Td)	Ref- erences	$(E/N)_{dc}$ (Td)
$\text{CCl}_4$	$720 \pm 60$	1370-8300	950	7,8	823
$\text{SiCl}_4$	$450 \pm 45$	540-3110	-	-	-
$\text{SF}_6$	$336 \pm 10$	390-2070	362	9	352
			355-360	7,8,10, 11	
$\text{CCl}_2\text{F}_2$	$312 \pm 14$	410-2490	345-385	12-17	358
$\text{CClF}_3$	$179 \pm 9$	250-1560	-	-	192
$\text{CF}_4$	$104 \pm 5$	160-620	135-149	18-22	149
$\text{O}_2$	$85 \pm 8$	140-830	108-119	23-28	116

The gases and vapors cited in Table 1 are listed in order of decreasing values of  $(E/N)_s$ . The third column in the table indicates the range of applied reduced field,  $E_0/N$ , which was used for each gas. The fourth column of Table 1 summarizes published values of reduced field,  $(E/N)_c$ , for which the ionization coefficient  $\alpha$  and attachment coefficient  $\beta$  are equal.<sup>7-28</sup> The range in values of  $(E/N)$  reflects the spread in these data. The value of  $(E/N)_c = 362$  Td obtained in Ref. 10 for  $\text{SF}_6$  (corrected for detachment is presently thought to be the most reliable.<sup>29,30</sup> No recent data were found for ionization and attachment coefficients in  $\text{CCl}_4$  and  $\text{SiCl}_4$ , and the available data for  $\text{SiCl}_4$  do not contain the intersection of the two coefficients.<sup>7,8</sup> The value of  $(E/N)_s = 450 \pm 45$  Td obtained in our measurements in  $\text{SiCl}_4$  may be viewed as an approximation for  $(E/N)_{dc}$  or the dielectric breakdown strength  $(E/N)_c$ . The last column of Table 1 presents literature values<sup>31</sup> for the dc breakdown field strength.

Our measurements of  $(E/N)_s$  produce values which are consistently smaller than the reduced field,  $(E/N)_c$ , at which  $\alpha = \beta$ , and lower than the breakdown field strength. The value  $(E/N)_c$  takes into account only electron production by impact ionization and electron loss by attachment (except that mentioned above for  $SF_6$  which is a detachment corrected value). In our discharge measurement, however, there are additional means of electron production; e.g., enhanced ionization due to a local space charge field.<sup>32</sup> Since this process tends to increase the ionization rate, the observed value of  $(E/N)_s$  is expected to be smaller than  $(E/N)_c$ . Similarly,  $(E/N)_s$  is expected to be smaller than  $(E/N)_{dc}$  because this additional process is not important at low values of applied field. One may also expect that the fast change from a high voltage across the gap during the formative phase to a much lower value during the discharge creates temporal nonequilibrium. This may cause further deviation from a simplified discharge model based on equilibrium ionization and attachment rates and drift velocity, consequently yielding a higher level of ionization than expected. The initial current rise beyond and settling to a constant level observed in  $CCl_4$  (see Figure 6) may be related to this temporal nonequilibrium. The effects of non-equilibrium between the external field and electron energy distribution as well as the question of applicability of transport coefficients in describing transient discharge behavior require further study.

The above measurements of  $(E/N)_s$  can be used to calculate the plasma resistance during the constant current discharge phase. Equation (1) may be rewritten in the following manner:

$$R_s = V_s / I_s = 2Z [1 / (1 - x_s) - 1] \quad (2)$$

where:

$$R_s \text{ is the plasma resistance, and } x_s = (E_0/N) / (E/N)_s \text{ is the ratio of incident field to } (E/N)_s$$

The plasma resistance,  $R_s$ , as a function of relative incident field, is shown in Figure 7 for two different transmission line impedance values,  $Z = 50\Omega$  and  $Z = 5\Omega$ . One may use values of  $(E/N)_s$  from Table 1

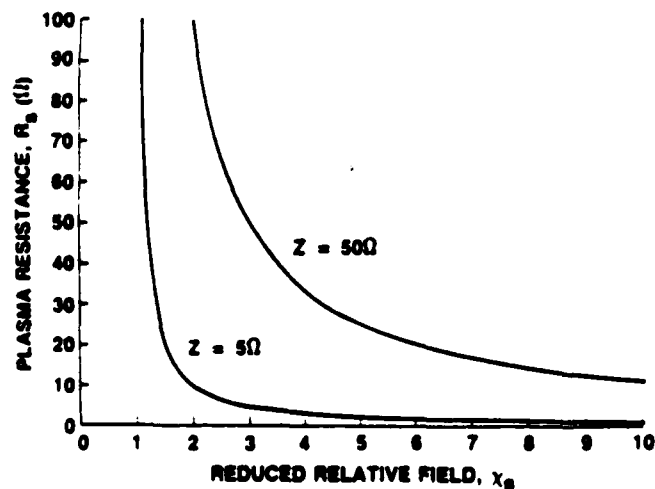


Figure 7. Plasma resistance,  $R_s$ , vs relative reduced field  $x_s = (E_0/N) / (E/N)_s$  for transmission line system with impedances  $Z=50\Omega$  and  $Z=5\Omega$ .

and find from Figure 7 the corresponding resistance for the chosen gas and incident reduced field value,  $E_0/N$ . In gases with high dielectric strength (characterized by high values of  $(E/N)_c$ ), low plasma resistance values may be achieved only at high field strength or low line impedance. This demonstrates the effect of the circuit impedance on plasma resistance and current in the glow phase. It should also be noted that for similar initial conditions, lower values of  $R_s$  are obtained in transient discharges than those predicted for dc breakdown.

This work was supported in part by the Office of Naval Research.

#### REFERENCES

1. W.W. Byszewski, M.J. Enright and J. M. Proud, IEEE Trans. Plasma Sci. **PS-10**, 281 (1982).
2. M.C. Cavenor and J. Meyer, Aust. J. Phys. **22**, 155 (1969).
3. M.M. Kekez, M.R. Barrault and J.D. Craggs, J. Phys. **D3**, 1886 (1970).
4. I.D. Chalmers, M. Duffy and D.J. Tedford, Proc. Roy. Soc. **A329**, 171 (1972).
5. W. Pfeiffer, IEEE Trans. on El. Insulation **EI-17**, 505 (1982).
6. D.F. Binns and R.J. Hood, Proc. IEE **116**, 1962 (1969).
7. R. Geballe and M.A. Harrison, Phys. Rev. **85**, 372 (1952).
8. L.B. Loeb, Basic Processes of Gaseous Electronics, Univ. of California Press, pp. 414-415 (1960).
9. L. E. Kline, D. K. Davies, C. L. Chen and P.J. Chantry, J. Appl. Phys. **50**, 6789 (1979).
10. M.S. Bhalla and J.D. Craggs, Proc. Phys. Soc. London **80**, 151 (1962).
11. T. Yoshizawa, Y. Sakai, H. Tagashira and S. Sakamoto, J. Phys. **D12**, 1839 (1979).
12. V.N. Maller and M.S. Naidu, Proc. Third IEE Int. Conf. on Gas Discharges, Vol. 1, London, 409 (1974).
13. H. A. Boyd, G. C. Crichton, and T. Munknielsen, Proc. First IEE Int. Conf. on Gas Discharges Vol. 1, London, 426 (1970).
14. C. Raja Rao and G.R. Govinda Raju, Int. J. Electron. **35**, 49 (1973).
15. M.A. Harrison and R. Geballe, Phys. Rev. **91**, 1 (1953).
16. J.L. Moruzzi, Brit. J. Appl. Phys. **14**, 938 (1963).
17. G.R. Govinda Raju and R. Hackam, J. Appl. Phys. **53**, 5557 (1982).
18. S.E. Bozin and C.C. Goodyear, Brit. J. Appl. Phys. **1**, 327 (1968).
19. I.M. Bortnik and A.A. Panov, Sov. Phys. Tech. Phys. **16**, 571 (1971).

20. M.S. Naidu and A.N. Prasad, J. Phys. D5, 983 (1972).
21. C. S. Lakshminarasimha, J. Lucas and D. A. Price, Proc. IEE 120, 1044 (1973).
22. C. S. Lakshminarasimha, J. Lucas and R. A. Snelson, Proc. IEE 122, 1162 (1975).
23. K. Masek, T. Ruzicka and L. Laska, Czech. J. Phys. B27, 888 (1977).
24. D. A. Price, J. Lucas and J. L. Moruzzi, J. Phys. D5, 1249 (1972).
25. D.A. Price and J.L. Moruzzi, J. Phys. D6, C17 (1973).
26. D.A. Price, J. Lucas and J.L. Moruzzi, J. Phys. D6, 1514, (1973).
27. S.A. Lawton and A.V. Phelps, J. Chem. Phys. 69, 1055 (1978).
28. D.T.A. Barr and M.W. Whittington, J. Phys. D8, 405 (1975).
29. JILA Information Center Report No. 22, Univ. of Colorado (1982).
30. 1981 Annual Report: Technical Assistance for Future Insulation Systems Research, NBSIR 8-2555, Nat. Bureau of Standards, Washington (1982).
31. J.C. Devins, IEEE Trans. on El. Insulation EI-15, 81 (1980). For O<sub>2</sub> see: K.P. Brand, IEEE Trans. on El. Insulation, EI-17, 451 (1982).
32. This uniformity may be destroyed by space-charge effects during the course of a discharge-- see, e.g.: W.W. Byszewski, G. Reinhold, Phys. Rev. A26, 2826 (1982), and E.E. Kunhardt and W.W. Byszewski, Phys. Rev. A21, 2096 (1980).

TRANSIENT GAS DISCHARGES IN  
PERFLUOROCARBONS

W.W. Byszewski, M.J. Enright, J.M. Proud  
GTE Labs Inc., Waltham, MA 02254

Transient gas discharges in  $CF_4$ ,  $C_2F_6$  and  $C_3F_8$  and their mixtures with argon have been studied experimentally. A pulse transmission line system was used to overvolt a test gap in order to attain breakdown within a short voltage pulse of 50-100ns. External UV radiation was used to eliminate statistical lag time. Formative time as a function of applied reduced field,  $E_0/N$ , and gas pressure, was measured and used in the determination of the effective ionization rates in the above mixtures. The reduced field at zero effective ionization rate,  $(E/N)_s$ , a value which is approximately equal to the dc dielectric strength,  $(E/N)_{dc}$ , has been determined from transmitted current waveforms. A uniform field model of the gas discharge<sup>1</sup> has been applied to predict current waveforms and values of  $(E/N)_s$  theoretically.

Perfluorocarbons, as strongly attaching gases, exhibit high dielectric strength. These gases also possess interesting transport properties which may be of interest in diffuse discharge switches.<sup>2</sup> This paper describes an efficient technique for developing data concerning the electrical insulating properties of such gases.

This work was supported in part by the Office of Naval Research.

---

<sup>1</sup> W.W. Byszewski, M.J. Enright, J.M. Proud, IEEE Transition Plasma Sci. PS-10, 281 (1982).

<sup>2</sup> L.G. Christophorou, S.R. Hunter, J.G. Carter, R.A. Mathis, Appl. Phys. Lett, 41, 147 (1982).

J-1     Formation and Decay of Nanosecond Discharges in  
Electron Attaching Gases,\* W.W. BYSZEWSKI,  
M.J. ENRIGHT, J.M. PROUD, GTE Labs, Inc., Waltham, MA --  
Experimental and theoretical investigations of the for-  
mation and decay of transient electrical discharges in  
electronegative gases will be reviewed. Phases of the  
discharge to be discussed include: the formation period,  
the period of voltage collapse, the phase where the  
electron production is balanced by electron attachment  
loss, the transition from glow to arc discharge condi-  
tions, and the decay of the plasma after the applied  
voltage has been terminated. Different electrical pro-  
perties of molecular gases can be deduced from studies  
of each of these phases. Experimental results obtained  
in a pulse transmission line system in several attaching  
gases and in nitrogen will be presented. Two simple  
theoretical models have been developed to predict cur-  
rent waveforms and good agreement with experimental data  
has been achieved for the first three phases of the dis-  
charge. Later phases will require more complex model-  
ing.

\*Work supported in part by the Office of Naval Research  
and by the Naval Surface Weapons Center.

In low electronegative gases carbon tetrafluoride ( $CF_4$ ), hexafluoroethane ( $C_2F_6$ ), perfluoropropane ( $C_3F_8$ ) and sulfurhexafluoride ( $SF_6$ ). Experimental results are compared with published empirical data and discrepancies are briefly analyzed.

## EXPERIMENT

The experiment system used in these studies was described in detail previously (Byzrewski, Enright and Proud, 1982) and is illustrated in Fig. 1. The experimental arrangement utilizes a 500 $\mu$  pulse

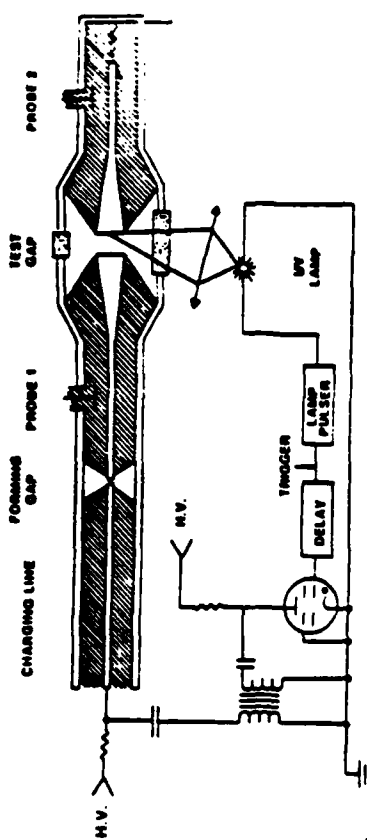


Fig. 1 - Schematic diagram of pulse transmission line system.

transmission line in which an approximately rectangular (45 ns), high voltage waveform, with 1.5 ns rise time is applied to the test gap. The plane-parallel, polished, stainless steel electrodes (4.4 cm dia) with Rogowski profile are used to provide uniform field conditions. The gas pressure in the gap is controlled within the range from 100 Torr up to 1 atm. The statistical component in the breakdown time lag is eliminated by means of UV flash illumination of the cathode surface (Felsenstein and Proud, 1985). The trigger system, synchronized with the UV flash, provides an almost instantaneously overvolted condition in the presence of initial free electrons in the gap.

A typical transmitted current waveform monitored with a capacitive divider probe and recorded by a fast transient digitizer is shown in Fig. 2. It consists of a prompt, low amplitude pulse due to charge displacement current charging the gap capacitance, followed by a delayed rise in the current. The time lag from the beginning of the capacitive spike to a measurable current level<sup>(1)</sup> is used in this paper as an experimental definition of a formative time lag.

The observed current waveforms in attaching gases exhibits a brief pause in the current growth shortly following the formative period (Fig. 2). This corresponds to the point in current development when the voltage between electrodes collapses, due to current rise in the gap to the value at which electron production and loss rates are balanced maintaining glow condition. The reduced field value at that period may be approximately predicted by simple uniform field model (Byzrewski, Enright and Proud, 1983a). Thereafter, the current rises to a value limited by the external circuit impedance. The low plasma resistance at this stage indicates the initial stage of an arc condition. Results in this paper are confined to the formative period and to the rate of the current rise which immediately follows formative period.

(1) For measurements reported here, in the range of applied voltage 25 kV - 30 kV this current level,  $I_c$  was fixed at 10A.

## NET IONIZATION RATES IN ELECTRONEGATIVE GASES

W.W. Byzrewski, M.J. Enright and J.M. Proud

GTE Laboratories, Inc.  
40 Sylvan Road  
Waltham, MA 02254

### ABSTRACT

Transient discharge development in electron-attaching gases has been investigated. Measurements of breakdown formative time lag and current waveforms in a transmission line pulse system were undertaken for carbon tetrafluoride ( $CF_4$ ), hexafluoroethane ( $C_2F_6$ ), perfluoropropane ( $C_3F_8$ ) and sulfurhexafluoride ( $SF_6$ ). A simple uniform field model has been employed to relate the formative time lag and the rate of current rise with the net ionization rate as a function of reduced electrical field above the breakdown limit. This transient technique appears very useful for the investigation of gas properties during breakdown formation under pulsed conditions.

### KEYWORDS

Net ionization rates; breakdown formative time lag; transient and pulsed gas discharges; electrical breakdown in gases; electronegative gases; gaseous insulators.

### INTRODUCTION

Breakdown time lag and net ionization rate data in gases, gas mixtures or vapors may be obtained from investigation of transient gas discharges (Byzrewski, Enright and Proud, 1982, 1983a). The measurements reported here have been obtained in a transmission line system which provides pulsed overvolted conditions with nanosecond rise time to a gas contained in a test gap. This arrangement and the range of experimental conditions simulate typical situations of pulse breakdown in gaseous insulators and high power switches.

Since the data are obtained under discharge conditions, their relevance to the above applications is enhanced over the prediction of discharge modeling based on cold gas data. The present results are thought to be influenced by modification of gas composition, multistep ionization, plasma radiation and other disturbed gas features which are normally overlooked in modeling. Evidence of the impact of these processes is seen in the discrepancy between calculated ionization rates based on single step ionization, attachment and recombination with data derived from transient waveform measurements (Byzrewski, Enright and Proud, 1983a). Similarly, potential drops during the glow phase of transient discharges are slightly lower than the values predicted from empirical coefficients (Byzrewski, Enright and Proud, 1983a). Therefore, data from transient discharge measurements, a technique which is a nonprocess-selective one, may better serve in studies of gaseous insulators and switches.

In the present paper we report data for breakdown time lags and net ionization rates measured

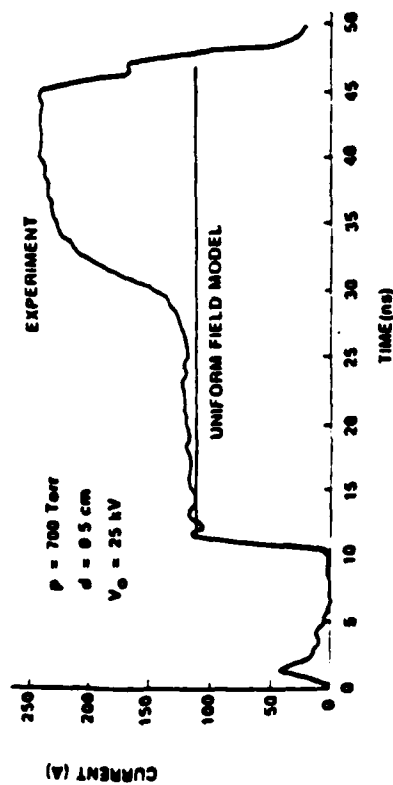


Fig. 2 - Current waveform in CF<sub>4</sub>.

### RESULTS

In order to obtain values for net ionization rates from formative time data we employed a simplified electron continuity equation under uniform field conditions:

$$d(n/dt) = kNn \quad (1)$$

where  $k$  is the net ionization rate,  $N$  the neutral particle density and  $n$  is the electron density. During the formative time,  $\tau$ , the field in the gap remains constant as the total current in the external circuit is small. Equation (1) may be easily integrated from  $t = 0$  to  $t = \tau$  leading to the following relation:

$$k = \ln(i_0/i_0) / \tau N \quad (2)$$

where  $i_0$  and  $i_1$  represent the current at the beginning and the end of the formative period. (2) From the measurements of the formative time lag,  $\tau$ , as a function of applied reduced field,  $E/N$ , gas number density,  $N$ , and electrode separation,  $d$ , we calculated net ionization rate,  $k$ , using the above relation. In Figs. 3 and 4 are shown results for net ionization rates in CF<sub>4</sub>, C<sub>2</sub>F<sub>6</sub> and C<sub>3</sub>F<sub>8</sub>. Results are plotted against the reduced field,  $E/N$ , for three values of electrode separation,  $d = 0.5, 1.0$  and  $1.5$  cm. The solid lines represent net ionization rates defined as a difference between ionization and attachment rates given by Naidu and Prasad (1972). Conclusions from the comparison of these results should be made with some caution since particular experimental conditions may not be well represented by single step ionization and attachment processes defining net ionization rate in this comparison. Nevertheless, our measurements at high values of  $E/N$  are much smaller than data by Naidu and Prasad (1972). Their results were obtained at low pressure range,  $p < 2$  Torr and an increase of attachment rate in C<sub>3</sub>F<sub>8</sub> with pressure has been reported. Beyond 2 Torr the attachment rate becomes independent of pressure (Naidu and Prasad, 1972). Lower net ionization rate observed in our high pressure experiment ( $p \geq 100$  Torr) than low pressure literature data, Figs. 3 and 4, may however indicate similar tendency at higher pressure range. The pressure dependence is in our representation difficult to follow since the increase of  $E/N$ , for given electrode separation, has been achieved by the pressure decrease.

The discrepancy between our pulsed, high pressure data and low pressure Naidu and Prasad (1972) results need further investigations. Although recent studies by Spyron, Sauers and Christophorou

(2)  $i_0$  is determined by a number of initial electrons produced by UV lamp estimated here as  $10^4$  el/cm<sup>2</sup> and therefore approximately  $i_0 = 10^{-7}$  A, for  $i_1$  see footnote (1)

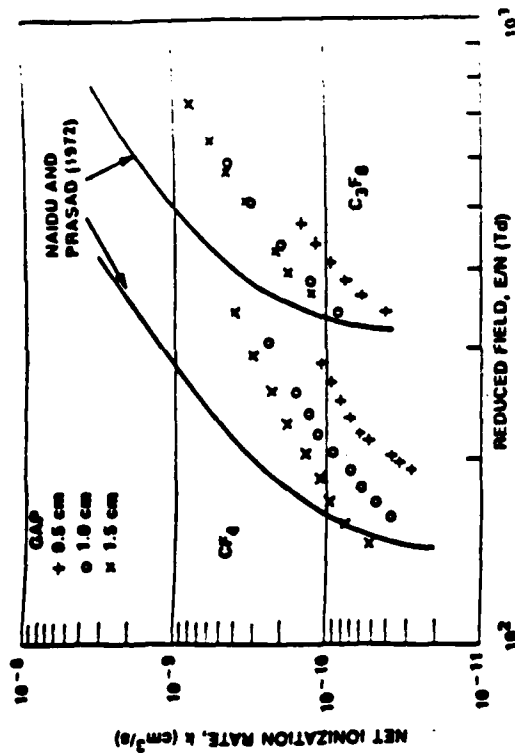


Fig. 3 - Net ionization rates in CF<sub>4</sub> and C<sub>3</sub>F<sub>8</sub>. Solid lines derived from Naidu and Prasad (1972).

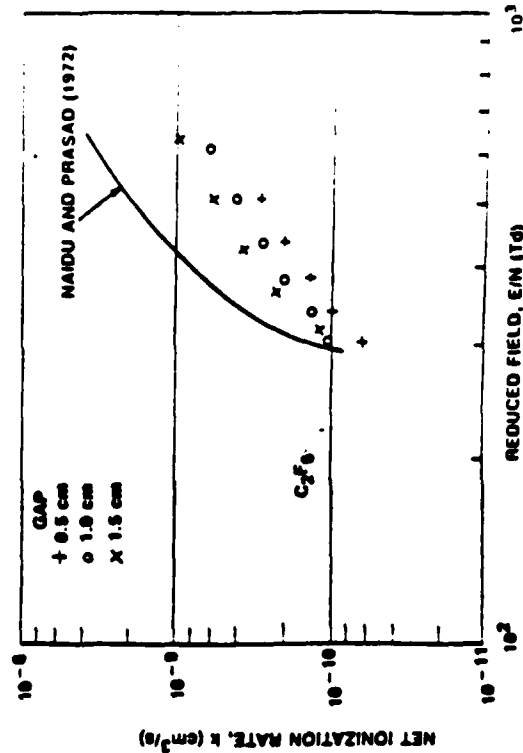


Fig. 4 - Net ionization rate in C<sub>2</sub>F<sub>6</sub>. Solid line derived from Naidu and Prasad (1972).

(1993) indicate that  $F^-$  is a main negative ion produced by electron attachment to  $CF_4$ ,  $C_2F_6$  and  $C_3F_8$  molecules, the processes involved are complex and results may well depend on the discharge pulse length and the gas pressure. Experimental effects may be ruled out here as responsible for lowering the net ionization rates since measurements in nonattaching gases such as  $N_2$ , He, Ne, Ar (Byszewski, Enright and Proud, 1983a) agreed well with published data in some cases and exceeded them in others.

A finite rise time in the incident voltage waveform may affect the measured formative time. Results in perfluorocarbons shown in Figs 3 and 4 are not affected substantially by finite incident voltage rise time since only long formative time lags have been collected. On the other hand the measurements in  $SF_6$  have been performed at higher field levels (short formative time lags). Therefore, the assumption that the gap is overvolted instantaneously fails under these circumstances. We used an effective value for incident reduced field,  $(E_0/N)_{eff}$  instead of a maximum value,  $E_0/N$ , in relation (3) formative time lag and net ionization rate vs  $E/N$ . We have defined the effective field  $(E_0/N)_{eff}$  through an average net ionization rate  $\langle k \rangle$  over the period  $T$ .

$$\langle k \rangle = \frac{1}{T} \int_0^T k(E_0/N) dt \quad (3)$$

where  $k(E_0/N)$  is the measured net ionization rate. In the integral instead of the maximum field  $E_0$  we take the field at any instant of the incident waveform,  $E_0(t)$ . The average net ionization rate  $\langle k \rangle$  obtained from Eq. (3) and measured relation  $k(E_0/N)$  defined the effective field.

$$k(E_0/N)_{eff} = \langle k \rangle \quad (4)$$

A couple of steps of iteration may be necessary to achieve self consistent  $k(E/N)$  relation. For effective use of the transient discharge technique presented here, however, the incident voltage rise time should be minimized. For calculations of effective field in  $SF_6$ , literature data for  $k(E/N)$  by Kline and co-workers (1979) and Maller and Naidu (1976) have been used in both Eqs. (3) and (4).

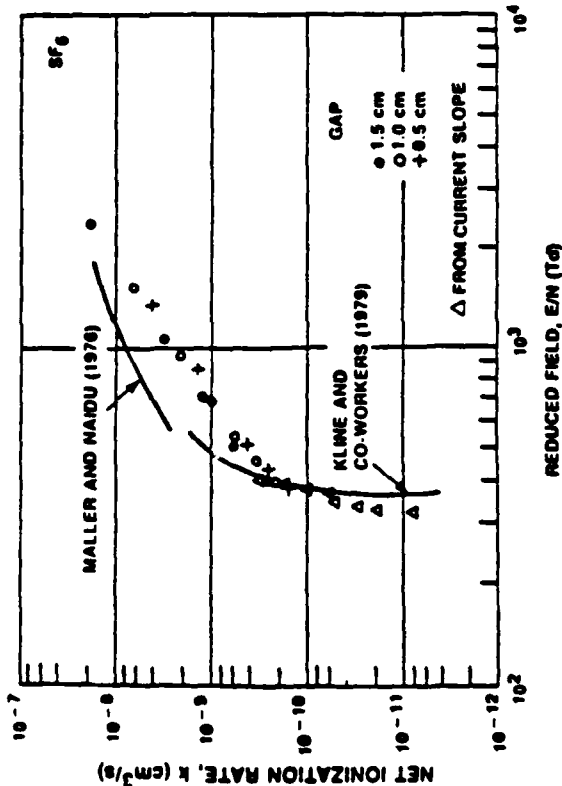


Fig 5 - Net ionization rate in  $SF_6$  as a function of effective reduced field  $\langle E/N \rangle$  corrected in accordance to Eqs. (3) and (4).

Results for the net ionization rates as a function of effective reduced field in  $SF_6$  are shown in Fig 5. The evident discrepancy between our results and those based on data by Kline and co-workers (1979) and by Maller and Naidu (1976) in addition to effects discussed above, may be associated with the effective field calculations for which precise determination of  $\tau$  at high overvoltage becomes essential.

The net ionization rate may also be determined from the slope of the current rise, which for low overvoltages is slow enough to be observed with the finite resolution of our detecting system. When the drift velocity can be approximated by a linear function of reduced field, the continuity equation for electrons [Eq. (1)] may be written in the following form:

$$k = (1/N) \frac{d(nj_0 \delta - ij_0 \delta)}{dt} \quad (5)$$

where  $\delta$  is a constant which depends on gas properties and experimental conditions. To obtain this relation between net ionization rate and the derivative of the current rise we also employed a circuit equation for the transmission line system and an expression for current in uniform field (Byszewski, Enright and Proud, 1982). By measuring the value of the current and its derivative at each instant during the initial phase of current rise, we determined the net ionization rate at that instant. Measuring also the voltage between electrodes at that instant we were able to relate net ionization rates to the reduced field. Results for  $SF_6$  have been obtained only at low overvoltages, the range limited by the resolution of detecting system, and are displayed in Fig 5. In this range of  $E_0/N$ , agreement with published data is observed.

The comparison of our results with published data for the net ionization rates underlines the importance of gas modification by the discharge itself. Further studies of temporal and pressure dependence of negative ion formation and dissociation are required for better understanding the observed discrepancy. Other loss processes in addition to attachment may also become significant. Nonuniform initial electron distribution in attaching gases seems to be responsible in part for smaller net ionization rates (longer formative time lags). This effect would be more pronounced at higher values of  $E/N$ . The transient discharge technique seems to be a very useful and appropriate technique in the study of plasma properties under the pulsed conditions which are typical for breakdown in gaseous insulators and high power switches.

The work was supported in part by the Office of Naval Research.

#### REFERENCES

Byszewski, W.W., M.J. Enright and J.M. Proud (1982). Transient development of nanosecond gas discharges. *IEEE Trans. Plasma Sci.*, **PS-10**, 281-285.  
 Byszewski, W.W., M.J. Enright and J.M. Proud (1983a). Net ionization rates measured by transient techniques. In *Proc. 16th Int. Conf. on Phenom. in Ion Gases*, Dusseldorf, Vol. 2, pp. 146-147.  
 Byszewski, W.W., M.J. Enright and J.M. Proud (1983b). EN in transient gas discharges. In *Proc. 4th IEEE Int. Pulsed Power Conf.*, Albuquerque, in press.  
 Feinthal, P. and J.M. Proud (1965). Nanosecond pulse breakdown in gases. *Phys. Rev. A*, **1**, 179, A1796-A1804.  
 Kline, L.E., D.K. Davies, C.L. Chen and P.J. Chanry (1979). Dielectric properties for  $SF_6$  and  $SF_6$  mixtures predicted from basic data. *J. Appl. Phys.* **50**, 6789-6796.  
 Maller, V.N. and M.S. Naidu (1976). Sparking potentials and ionization coefficients in  $SF_6$ . *Proc. IEEE*, **123**, 107-108.  
 Naidu, M.S., A.N. Prasad (1972). Mobility, diffusion and attachment of electrons in perfluorocarbons. *J. Phys. D*, **5**, 983-993.  
 Spyrou S.M., I. Savaris and I.G. Christophorou (1983). Electron attachment to the perfluoroalkanes  $n-C_nF_{2n+2}$  and  $C_4O_{10}$ . *J. Chem. Phys.* **78**, 7200-7216.

END

FILMED

2-86

DTIC